

Dynamic Graph-Based Anomaly Detection in the Electrical Grid

Shimiao Li, *Graduate Student Member, IEEE*, Amritanshu Pandey, *Member, IEEE*, Bryan Hooi, *Member, IEEE*, Christos Faloutsos, *Member, IEEE*, and Larry Pileggi, *Fellow, IEEE*

Abstract—Given sensor readings over time from a power grid, how can we accurately detect when an anomaly occurs? A key part of achieving this goal is to use the network of power grid sensors to quickly detect, in real-time, when any unusual events, whether natural faults or malicious, occur on the power grid. Existing bad-data detectors in the industry lack the sophistication to robustly detect broad types of anomalies, especially those due to emerging cyber-attacks, since they operate on a single measurement snapshot of the grid at a time. New ML methods are more widely applicable, but generally do not consider the impact of topology change on sensor measurements and thus cannot accommodate regular topology adjustments in historical data. Hence, we propose DYNWATCH, a domain knowledge based and topology-aware algorithm for anomaly detection using sensors placed on a dynamic grid. Our approach is accurate, outperforming existing approaches by 20% or more (F-measure) in experiments; and fast, averaging less than 1.7ms per time tick per sensor on a 60K+ branch case using a laptop computer, and scaling linearly with the size of the graph.

Index Terms—anomaly detection, dynamic grid, graph distance, LODE, power system modeling

I. INTRODUCTION

Maintaining and improving the reliability of the electric power grid is a critically important goal. Estimates [1] suggest that reducing outages in the U.S. grid could save \$49 billion per year, reduce emissions by 12 to 18%, while improving efficiency could save an additional \$20.4 billion per year. Although grid operators and engineers work tirelessly to maintain reliability of the electric grids, many challenges persist. Climate change is increasing the frequency of natural disasters, resulting in higher rate of equipment failure. Adding to the climate risk is a new adversary in the form of cyber-intrusions that is capable of disrupting grid control and communication. This is evident from the recent reports of foreign hackers successfully penetrating control rooms of the U.S. power plants [2] and of cyber-attacks on the Ukrainian grid in 2015-2016 [3] [4] that brought down sections of the network causing damages worth billions of dollars.

A key tool that the grid operators use to safeguard against these failures, whether naturally occurring or malicious, involves the anomaly detection capabilities that are implemented

Manuscript submitted to IEEE Transactions on Smart Grid.

S. L., A. P., and L. P. are with the Department of Electrical and Computer Engineering, Carnegie Mellon University, Pittsburgh, PA, 15213 USA (email: {shimiao, amritanp, pileggi}@andrew.cmu.edu), B. H. is with the School of Computing and the Institute of Data Science in National University of Singapore (email: bhooi@comp.nus.edu.sg), C. F. is with the Department of Computer Science, Carnegie Mellon University, Pittsburgh, PA, 15213 USA (email: christos@cs.cmu.edu)

in the grid control rooms. The primary purpose of these techniques is to help grid operators isolate faulty data from the healthy ones to result in accurate situational awareness, which further allows grid operators to take rapid corrective actions. In almost real-time, these methods can analyze measurement values, dynamics and other informative features to detect abnormal events including erroneous topology or measurements, while accommodating normal grid behaviors, including regular topology changes and power configuration adjustments.

In existing power grids, anomaly detection is performed within the Energy Management Systems (EMS) [5] that are installed in the control rooms. The EMS through Supervisory Control and Data Acquisition (SCADA) system collects two primary sources of data: i) online measurement data from various sensors such as remote terminal units (RTUs) and phasor measurement units (PMUs) and ii) status indicators and breaker positions for various devices such as lines and transformers. Taking these two classes of data as input, separate analysis units within the EMS are run to identify anomalies in measurements and topology data.

AC state-estimation (ACSE) [6] along with bad-data detection (BDD) algorithms [7] provide anomaly detection for measurement data from RTUs and PMUs. These are run every 1 to 10 minutes by solving an optimization problem and traditionally the residuals have been further used for BDD via hypothesis testing. The most widely used problem formulation is the weighted-least-square (WLS) form [7], minimizing mean-squared measurement error. Some other formulations are designed to achieve intrinsic robustness against bad data, including least absolute value (LAV) based [8], least median of squares based [9], as well as iteratively reweighted least-squares based approaches [10]. Unfortunately when RTUs are included, these methods generally suffer from difficult convergence due to non-convex measurement models. There have been recent attempts at convexification of the state-estimation problem [11] [12] [13] [14]; however, several limitations persist. These include inability to detect coordinated attacks like false-data injection attack and high sensitivity to network topology errors.

On the other hand, topology anomalies are detected by the network topology processor (NTP) [15] [16], which transforms the input circuit breaker/switching status data into the bus-branch model in which network connectivity and meter locations are identified. However, existing operational NTP does not account for topology errors due to erroneous status data corrupted by communication, operator entry errors, cyber-attacks, etc. As a countermeasure, there exist research

works that overcome some challenges of existing NTP. For instance, generalized topology processing [17] creates pseudo-measurements and applies hypothesis tests to detect topology anomalies. Another approach [18] applies hypothesis testing on WLS residuals from SE to detect topological errors, as an extended application of ACSE BDD. More recently, other advanced methods such as [19] [20] [12] have been developed where TE and ACSE are merged together to perform estimation using a bus-breaker model. This enables measurement error and topology error to be effectively identified and separated. However, challenges persist here as well, mostly due to the lack of efficient and scalable methods to handle the non-linearity with conventional measurements and the inability of these methods to detect topology anomalies during coordinated cyber-attacks.

These challenges with existing TE and ACSE can be addressed by using anomaly detection based on statistical behavior. Instead of analysing the well-defined measurement models in a snapshot, one can leverage statistical behaviors to extract some patterns from historical data. This can be helpful since most anomalies, either unexpected faults or cyber-attacks, usually disrupt the statistical consistency of the data stream, despite being invisible from one single snapshot. Existing behavioral anomaly detection methods can be broadly categorized into model-based (where an expectation of observation is obtained by fitting a mathematical model) [21] [22] [23], representation based [24] [25], graphical methods [26], and others (see Section II for related works). Generally, these families of methods are all directly applicable to the problem described in this paper. However, these methods either do not consider the impact of graph change on the observations [21] [23] [24], or assume a static topology across the data stream [27]. This is problematic for grid problems since different grid configurations naturally cause differences in grid measurements. Hence, previous observations from disparate topologies and loadings may provide little value in assessing the anomalousness at a given time t . Without a selection of relevant data, methods may produce more false positives by falsely creating alarms when regular topology changes occur.

To handle this, a more applicable way is to make the behavioral anomaly detection method *context-aware*, so that it indicates the expected patterns of behavior from data samples collected with relevant context of their topology. Hence, our paper proposes such a method that processes the time series of measurements and the time series of their topology. Intuitively, the method works by defining graph distances based on domain knowledge and estimating a reliable distribution of measurements at time t from the most relevant previous data. Then, an alarm is created if the measured value deviates greatly from the center of its distribution. The goal of the method is to directly consider the impact of topology on observations, so that regular topological changes are accommodated, while detecting any false measurement and topological errors. Furthermore, to account for large-scale grids, we develop a locally-sensitive variant, DYNWATCH-LOCAL.

The rest of the paper is organized as follows: Section II provides background of existing methods. Section III shows our proposed method. Section IV validates the method with

experiment results. Finally, Section V concludes the paper.

II. BACKGROUND AND RELATED WORK

A. Existing ML-based Anomaly Detection Approaches

a) Time Series Anomaly Detection: Numerous algorithms exist for anomaly detection in univariate time series [28]. For multivariate time series, LOF [24] uses a local density approach. Isolation Forests [26] partition the data using a set of trees for anomaly detection. Other approaches use neural networks [23], distance-based [29], and exemplars [30]. However, none of these consider the graph structure.

b) Anomaly Detection in Temporal Graphs: [31] finds anomalous changes in graphs using an egonet (i.e. neighborhood) based approach, while [32] uses a community-based approach. [33] finds connected regions with high anomalousness. [34] detects large and/or transient communities using Minimum Description Length. [35] finds change points in dynamic graphs, while other partition-based [36] and sketch-based [37] also exist for anomaly detection. However, these methods focus on detecting unusual communities or connections, while our approach has a very different goal of detecting disturbances which cause changes in sensor values.

c) Anomaly Detection with Domain Expert Knowledge: Domain specific anomaly detectors based on optimal power flow [38], SE BDI [7] and TE programs [15] [17] already exist and are purely based on power system theories, yet they are typically limited to specific disturbances and attacks against the grid components. On the contrary, ML methods, as illustrated above, are more generally applicable; however, without basic understanding of how the real world grid operates, they are likely to perform poorly. Motivated by the pros and cons, many efforts [27] [39] have combined the benefits of the two, embedding the domain-knowledge in general ML methods. Such methods with domain knowledge have been shown to have higher performance (see [27] [39]) but still do not fully consider the dynamic nature of the electric grid.

To summarize, the major contribution of DYNWATCH when compared with existing methods are summarized in table I.

TABLE I
COMPARISON OF RELATED APPROACHES: ONLY DYNWATCH SATISFIES
ALL THE LISTED PROPERTIES.

	Time Series	Graph-based	GridWatch	DYNWATCH
Graph Data	✓	✓	✓	✓
Anomalies in Sensor Data	✓	✓	✓	✓
Changing Graph	✓			✓
Locally Sensitive				✓

B. Handling Redundant Data

Transmission grids, in order to be observable, have a large number of RTUs and PMUs installed. For the anomaly detection algorithm developed in this paper, processing the

large volume of redundant data for anomaly detection is unnecessary and computationally prohibitive. This is because each sensor predominantly captures the relative information of its neighboring sensors as well. Therefore, to create a proper input for anomaly detection, pre-processing techniques can be deployed: Principal Component Analysis (PCA) [40] creates a low-dimensional representation by extracting uncorrelated directions; projection pursuit [41] reduces the input to a low-dimensional projected time series that optimizes the kurtosis coefficient; Independent Component Analysis (ICA) [42] identifies a subset of independent variables. Alternative techniques like cross-correlation analysis [43] also help create a low-dimensional input. A detailed survey regarding dimensionality reduction can be found in [44]. Rather than transforming the redundant input, other algorithms for sensor placement [45] are also applicable, by suggesting the best several locations of sensors to be installed and providing observability. [27] has shown the selection of a small number of sensor locations with provably near-optimal probability of detecting an anomaly.

C. Background: Line Outage Distribution Factor (LODF)

Line Outage Distribution Factor (LODF) is a sensitivity measure of how much an outage on a line affects real power flow on other lines in the system [46]. This factor can be easily and efficiently calculated by assuming a DC power flow model with lossless lines or a linearized AC power flow model around the operating point, and is commonly used to estimate the linear impact of line outage. For an outage on line k , LODF d_l^k gives the ratio between power change Δf_l on an observed line l and the pre-outage real power f_k on the outage line k .

$$d_l^k = \frac{\Delta f_l}{f_k}$$

III. PROPOSED DYNWATCH ALGORITHM

A. Preliminaries

Table II shows the symbols used in this paper.

TABLE II
SYMBOLS AND DEFINITIONS

Symbol	Interpretation
$\mathcal{G} = (\mathcal{V}, \mathcal{E})$	Input graph
\mathcal{S}	Subset of nodes to place sensors on
n	Number of nodes
s	Number of scenarios
\mathcal{N}_i	Set of edges adjacent to node i
$V_i(t)$	Voltage at node i at time t
$I_e(t)$	Current at edge e at time t
$s_{ie}(t)$	Power w.r.t. node i and edge e at time t
$\Delta s_{ie}(t)$	Power change: $\Delta s_{ie}(t) = s_{ie}(t) - s_{ie}(t-1)$
$X_i(t)$	Sensor vector for scenario i at time t

We are given a dynamic graph (grid) $\mathcal{G}_t = (\mathcal{V}(t), \mathcal{E}(t))$ at each time tick t , where $\mathcal{V}(t)$ denotes the set of nodes (active grid buses), and $\mathcal{E}(t)$ denotes the set of edges (active grid branches). Also we have a fixed set of sensors $\mathcal{S} \subseteq \mathcal{V}$. Each sensor installed on node i can obtain PMU or RTU measurements at each time t .

For each sensor on node i , we obtain the power flows on all lines adjacent to node i , as observed in [27] that using power (rather than current) provides better anomaly detection in practice. For any PMU bus i and edge $e \in \mathcal{N}_i$, define the power w.r.t. i along edge e as $s_{ie}(t) = V_i(t) \cdot I_e(t)^*$, where $*$ is the complex conjugate.

B. Motivation and Method Overview

Consider the simple power grid shown in Figure 1, which evolves over time from \mathcal{G}_1 to \mathcal{G}_2 to \mathcal{G}_3 . For simplicity, assume that we have a single sensor, from which we want to detect anomalous events. How do we evaluate whether the current time point ($t = 15$) is an anomaly? If the graph had not been changing, we could simply combine all past sensor values to learn a distribution of normal behavior (e.g. fitting a Gaussian distribution as in $\mathcal{N}_{t=15}$), then evaluate the current time point using this Gaussian distribution (e.g. in terms of number of standard deviations away from the mean).

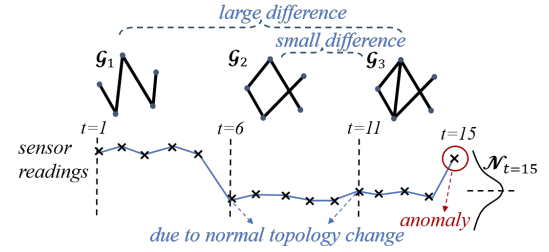


Fig. 1. Simple motivating example: anomaly detection under changing graphs using DYNWATCH.

In the changing graph setting, we still want to learn a model of normal behavior ($\mathcal{N}_{t=15}$), but while taking the graph changes into account. Note that \mathcal{G}_2 and \mathcal{G}_3 are only slightly different, while \mathcal{G}_1 and \mathcal{G}_3 are very different. Hence, the sensor values coming from \mathcal{G}_2 (i.e. time 6 to 10) should be taken into account more highly when constructing $\mathcal{N}_{t=15}$, as compared to those from \mathcal{G}_1 . Intuitively, the sensor values from \mathcal{G}_1 are drawn from a very different distribution from the current graph, and thus should not influence our learned model $\mathcal{N}_{t=15}$. In general, the more similar a graph is to the current graph, the more we should take its sensor values into account when learning our current model. This motivates the 3-step process we use:

- 1) **Graph Distances:** Measure the distance between each past graph and the current graph.
- 2) **Temporal Weighting:** Weight the past sensor data, where data from graphs that are similar to the current one is given higher weight.
- 3) **Anomaly Detection:** Learn a distribution of normal behavior (\mathcal{N}_t) from the weighted sensor values, and measure the anomalousness at the current time based on its deviation from this distribution.

In the following sections, we first introduce our domain-aware graph distance measure based on Line Outage Distribution Factors (LODF) [46]. Then, we describe our temporal weighting and anomaly detection framework, which flexibly allows for any given graph distance measure. Finally, we

present an alternate distance measure that is locally sensitive; i.e. it accounts for the local neighborhood around a given sensor.

C. Proposed Graph Distance Measure

In this section, we describe how we measure the distance $D(\mathcal{G}_i, \mathcal{G}_j)$ between any pair of graphs. For ease of understanding, the rest of Section III uses the example of anomaly detection at $t = 15$ in Figure 1 as an extended case study, but our approach can be easily extended to the general case.

Intuitively, our goal is for our graph distance to represent **redistribution of line power flow**. Critical changes in topology result in large redistribution of power. Thus, the graph distance arising from a topology change should be large if the changed edges can potentially cause large amounts of power redistribution.

Hence, given two graphs $\mathcal{G}_i(\mathcal{V}(i), \mathcal{E}(i))$ and $\mathcal{G}_j(\mathcal{V}(j), \mathcal{E}(j))$ with different topology, we first define a transition state which takes the union of the two graphs:

$$\mathcal{G}_{trans} = (\mathcal{V}(i) \cup \mathcal{V}(j), \mathcal{E}(i) \cup \mathcal{E}(j))$$

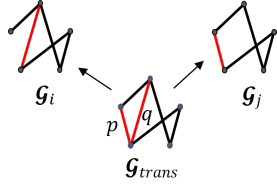


Fig. 2. Transition state of two graphs: the union of two graphs.

Then the topology changes from \mathcal{G}_i to \mathcal{G}_j can be considered as different line deletions from their base graph \mathcal{G}_{trans} . For each single line deletion, e.g. line p , we define its contribution x_p to graph distance by taking the average of its power impacts on all other lines as measured by LDF:

$$x_p = \frac{1}{|\mathcal{E}(i) \cup \mathcal{E}(j)|} \sum_{l \in \mathcal{E}(i) \cup \mathcal{E}(j) \setminus \{p\}} (|d_l^p|)$$

where $|\mathcal{E}(i) \cup \mathcal{E}(j)|$ denotes the cardinality of set $\mathcal{E}(i) \cup \mathcal{E}(j)$, d_l^p denotes the LDF coefficient with p as outage line and l as observed line.

Then graph distance $D(\mathcal{G}_i, \mathcal{G}_j)$ is given by summing up the contributions of different line deletions from the base graph:

$$D(\mathcal{G}_i, \mathcal{G}_j) = \sum_{p \in (\mathcal{E}(i) - \mathcal{E}(j)) \cup (\mathcal{E}(j) - \mathcal{E}(i))} x_p$$

where $\mathcal{E}(i) - \mathcal{E}(j) = \{p | p \in \mathcal{E}(i), p \notin \mathcal{E}(j)\}$ and accordingly, $(\mathcal{E}(i) - \mathcal{E}(j)) \cup (\mathcal{E}(j) - \mathcal{E}(i))$ denotes all the edge changes between the two graphs.

Intuitively, this definition uses LDF as a measure of the impact on power flow of the removal of line p . Hence, edges with high LDF to many other edges can potentially cause greater change in power flow, and thus our graph distance measure places greater importance on these edges.

D. Proposed Temporal Weighting Framework

In this section, we assume that we are given any distance measurements $D(\mathcal{G}_i, \mathcal{G}_j)$ between any pair of graphs \mathcal{G}_i and \mathcal{G}_j , and explain how to use them to assign weights to each previous sensor data. This procedure can take the LDF-based distance defined in the previous subsection as input, but also allows us to flexibly use any given graph distance measure. The proposed Temporal Weighting is given in Algorithm 1.

Algorithm 1: Temporal Weighting Framework at time $t = 15$ (see example in Figure 1)

Input: Graph distance $D(\mathcal{G}_1, \mathcal{G}_3)$, $D(\mathcal{G}_2, \mathcal{G}_3)$, $D(\mathcal{G}_3, \mathcal{G}_3)$; sensor data $s_i(t)$ with $t = 1, 2, \dots, 15$, $i = 1, 2, \dots, N_{sensor}$.

Output: Anomaly score $A(15)$.

1 Extend graph distance to tick-wise distance. Each previous time tick is given a distance d_t according to the graph it comes from:

$$d_t = \begin{cases} D(\mathcal{G}_1, \mathcal{G}_3) & \text{for } t = 1, 2, \dots, 5 \\ D(\mathcal{G}_2, \mathcal{G}_3) & \text{for } t = 6, 7, \dots, 10 \\ D(\mathcal{G}_3, \mathcal{G}_3) & \text{for } t = 11, \dots, 14 \end{cases}$$

2 Temporal Weighting: Use d_1, \dots, d_{14} to assign weights w_1, \dots, w_{14} to the past sensor data using Algorithm 2.

For the purpose of utilizing previous data from a series of dynamic graphs, **Temporal Weighting** plays an important role. The resulting weights directly determine how much information to extract from each previous record, thus requiring special care. Intuitively, the weights should satisfy the following principles:

- The larger the distance d_t , the lower the weight w_t . This is because high d_t indicates that time tick t is drawn from a very different graph from the current one, and thus should not be given high weight when estimating the expected distribution at the current time
- Positivity and Normalization: $\sum_t w_t = 1, w_t \geq 0$

To satisfy these conditions, we use a principled optimization approach based on **bias-variance trade-off**. Intuitively, the problem with using data with high d_t is **bias**: it is drawn from a distribution that is very different from the current one, and that can be considered a biased sample. We treat d_t as a measure of the amount of bias. Hence, given weights w_1, \dots, w_{14} on previous data (in Figure 1 example), the total bias we incur can be defined as $\sum_{t \in \{1, \dots, 14\}} w_t d_t$.

We could make the bias low simply by assigning positive weights to only time points from the most recent graph. However, this is still unsatisfactory as it results in a huge amount of **variance**: since very little data is used to learn $N_{t=15}$, the resulting estimate has high variance. Multiplying a fixed random variable by a weight w_t scales its variance proportionally to w_t^2 . Hence, given weights $w = [w_1, w_2, \dots]$, the total amount of variance is proportional to $\frac{1}{2} w^T w$, which we define as our variance term.

We thus formulate the following optimization problem as minimizing the sum of bias and variance, thereby balancing

the goals of low bias (i.e. using data from similar graphs) and low variance (using sufficient data to form our estimates). We formulate the problem as:

$$\min_w \sum_t w_t d_t + \frac{1}{2} w^T w$$

subject to

$$\begin{aligned} \sum_t w_t &= 1 \\ w_t &\geq 0, \forall t \end{aligned}$$

By writing out its Lagrangian function:

$$L(w, \lambda, u) = d^T w + \frac{1}{2} w^T w + \lambda(1 - \sum_t w_t) - u^T w$$

and applying KKT conditions, we can see the optimal primal-dual solution (w, λ^*, u^*) must satisfy:

$$d_t + w_t - \lambda^* - u_t^* = 0$$

Since we have $d_t \geq 0$, by further manipulation we have:

$$w_t = \max\{\lambda^* - d_t, 0\}$$

Moreover, there is a unique choice of λ^* such that the resulting weights w_t sum up to 1. This w_t against d_t relationship is shown in Figure 3. This result is intuitive: as d_t increases, the resulting weight we assign w_t decreases, and if d_t passes a certain threshold, it becomes large enough so that any reduction in variance it could provide is more than offset by its large bias, in which case we assign it a weight of 0.

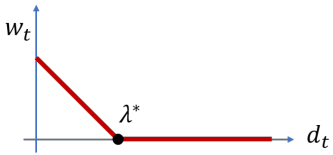


Fig. 3. $w_t - d_t$ relationship.

Our Temporal Weighting algorithm is in Algorithm 2.

Algorithm 2: Computing Temporal Weights w_t

Input: distance d_t , with $t = 1, 2, \dots, N$

Output: weights w_t , with $t = 1, 2, \dots, N$

1 Compute the unique λ^* that satisfies:

$$\sum_{t \in \{1, 2, \dots, N\}} \max\{\lambda^* - d_t, 0\} = 1$$

2 Get weights w_t :

$$w_t = \max\{\lambda^* - d_t, 0\}$$

E. Proposed Anomaly Detection Algorithm

Having obtained our weights w_t , the remaining step is to compute our anomaly score, as shown in Algorithm 3.

We focus on 3 metrics from sensor data as indications of power system anomalies. These metrics were studied in [27] and found to be effective for detecting anomalies in power grid sensor data. In our setting, recall that for each sensor, we can obtain Δs_i that contains changes of real and reactive power on the adjacent lines, over time. The 3 metrics are:

- **Edge anomaly metric:** $X_{edge,i}(t) = \max_{l \in E_{adj}} \Delta s_{i,l}$ which measures the maximum line flow change among lines connected to the sensor. Let E_{adj} denote the set of lines connected to sensor i :
- **Average anomaly metric:** $X_{ave,i}(t) = \text{mean}\{\Delta s_{i,l} \mid l \in E_{adj}\}$, which measures the average line flow change on the lines connected to the sensor:
- **Diversion anomaly metric:** $X_{div,i}(t) = \text{std}\{\Delta s_{i,l} \mid l \in E_{adj}\}$, which measures the standard deviation of line flow change over all lines connected to the sensor:

Intuitively, for each metric, we want to estimate a model of its normal behavior. To do this, we compute the weighted median and interquartile range (IQR)¹ of the detection metric, weighting the time points using our temporal weights w_1, \dots, w_t . We can then estimate the anomalousness of the current time tick by computing the current value of a metric, then subtracting its weighted median and dividing by its IQR. The exact steps are given in Algorithm 3.

Algorithm 3: Anomaly Detection (see Figure 1)

Input: Temporal weights w_t ; sensor data $s_i(t)$ with $t = 1, 2, \dots, 15$, $i = 1, 2, \dots, N_{sensor}$

Output: anomaly score $A(15)$

- 1 **for** $i \leftarrow 1$ to N_{sensor} **do**
- 2 **Compute weighted median and IQR:**
- 3 $\mu_{edge} = \text{Weighted Median}\{X_{edge,i}(t) \mid t = 1, \dots, 14\}$
- 4 $IQR_{edge} = \text{Weighted IQR}\{X_{edge,i}(t) \mid t = 1, \dots, 14\}$
- 5 weighted by w_1, \dots, w_{14} (similarly for X_{ave}, X_{div}).
- 6 **Calculate sensor-wise anomaly score at t=15:**
- 7 $a_i(15) = \max_{metric \in \{edge, ave, div\}} \frac{X_{metric,i}(15) - \mu_{metric}}{IQR_{metric}}$
- 8 **Calculate anomaly score for target time tick**, as the max score over sensors:

$$A(15) = \max_{i \in \{1, \dots, N_{sensor}\}} a_i(15)$$

F. Proposed Locally Sensitive Distance Measure

Motivation: In the previous section, we computed a single distance value $D(\mathcal{G}_i, \mathcal{G}_j)$ between any pair of graphs. However, consider two graphs \mathcal{G}_i and \mathcal{G}_j in Figure 4 that are very

¹IQR is the difference between 1st and 3rd quartiles of a distribution, and is commonly used as a robust measure of spread.

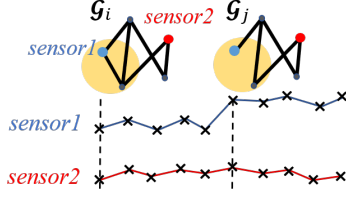


Fig. 4. Simple motivating example: DYNWATCH-LOCAL. The two graphs are very different within the yellow localized region. However, sensor 2 is far away from the yellow region and thus experiences no changes.

different due to a small yellow localized region (e.g. in a single building which underwent heavy renovation). Hence, $D(\mathcal{G}_i, \mathcal{G}_j)$ is large, indicating not to use data from \mathcal{G}_i when we analyse a time tick under \mathcal{G}_j . However, from the perspective of a single sensor s (sensor 2) far away from the localized region, this sensor may experience little or no changes in the power system's behavior, so that data from graph \mathcal{G}_i may have a similar distribution as data from graph \mathcal{G}_j , and so for this sensor (sensor 2) we can still use data from \mathcal{G}_i to improve anomaly detection performance. Hence, rather than computing a single distance $D(\mathcal{G}_i, \mathcal{G}_j)$, we compute a separate **locally-sensitive** distance $D_s(\mathcal{G}_i, \mathcal{G}_j)$ specific to each sensor, which measures the amount of change between graphs \mathcal{G}_i and \mathcal{G}_j in the 'local' region to sensor s . Clearly, the notion of 'local regions' must be carefully defined: we will define them based on LODF, recalling that LODF measures how much changes on one edge affect each other edge.

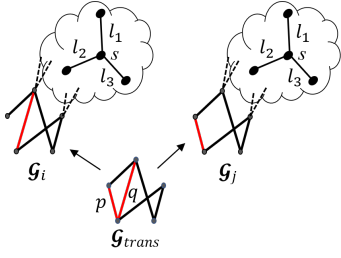


Fig. 5. Local graph distance: the adjacent lines connected to each sensor s are considered.

Intuitively, the local distance between two graphs with respect to sensor s is large if the changed edges can potentially cause large power change nearby the sensor. Hence, given two graphs $\mathcal{G}_i(\mathcal{V}(i), \mathcal{E}(i))$ and $\mathcal{G}_j(\mathcal{V}(j), \mathcal{E}(j))$ with their transition state \mathcal{G}_{trans} and a sensor s of interest, the local graph distance contribution y_p of line p with respect to sensor s can be calculated by multiplying the whole-grid-wide contribution x_p with a weighing factor c_p^s . This c_p^s coefficient filters the power impact for sensor s using the maximum power impact of line deletion on lines around this sensor:

$$c_p^s = \max_{l \in \mathcal{E}_{sensor}(s)} |d_l^p|$$

$$y_p = x_p c_p^s$$

where $\mathcal{E}_{sensor}(s)$ denotes the set of edges around sensor s (e.g. in Figure 5, $\mathcal{E}_{sensor}(s) = \{l_1, l_2, l_3\}$), and d_l^p denotes the LODF with p as outage line and l as observed line.)

Then, as before, the local graph distance with respect to sensor s is defined by summing up the local graph distance contributions of different line deletions from the graph:

$$D_s(\mathcal{G}_i, \mathcal{G}_j) = \sum_{p \in (\mathcal{E}(i) - \mathcal{E}(j)) \cup (\mathcal{E}(j) - \mathcal{E}(i))} y_p$$

IV. EXPERIMENTS

We design experiments to answer the following questions:

- **Q1. Anomaly Detection Accuracy:** how accurate is the anomaly detection from our method compared to baselines?
- **Q2. Scalability:** how do our algorithms scale with the graph size?

Our code and data are publicly available at <https://github.com/bhooi/dynamic.git>. Experiments were done on a 1.9 GHz Intel Core i7 laptop, 16 GB RAM running Microsoft Windows 10 Pro.

Case Data: We use 2 test cases: CASE2383 is an accurate reconstruction of part of the European high voltage network, and ACTIVSG25K is a synthetic network that mimics the Texas high-voltage grid in the U.S. The ACTIVSG25K represents a similar sized system as the PJM (the largest independent service operator (ISO) in the U.S.) grid, which contains around 25 to 30k buses [47].

Selection of sensors: Section II documents various methods that can select the set of optimal sensors for the proposed method. To be conservative, for these experiments, we select random subsets of sensors (of varying sizes) as input. The good performance even with randomly selected sensor measurements validates the effectiveness of our method in selecting relevant time frames from historical data.

A. Q1. Anomaly Detection Accuracy

In this section, we compare DYNWATCH against baseline anomaly detection approaches, while varying the number of sensors in the grid.

Experimental Settings: Starting with a particular test case as a base graph G , we first create 20 different topology scenarios where each of them deactivates a randomly chosen branch in the based graph. These subsequent 20 network topologies represent the dynamic grid with topology changes due to operation and control. Then for each topology scenario, we use MatPower [47], a standard power grid simulator, to generate 60 sets of synthetic measurements based on the load characteristics described in the following paragraph. As a result, the multivariate time series with $20 \times 60 = 1200$ time ticks mimics the real-world data setting where sensors receive measurements at each time tick t , and the grid topology changes every 60 time ticks. Finally, we sample 50 random ticks out of 1200 as times when anomalies occur. Each of these anomalies is added by randomly deleting an edge on the corresponding topology.

Following [27], to generate an input time series of loads (i.e. real and reactive power at each node), we use load patterns estimated from real data [48] recorded from the Carnegie Mellon University (CMU) campus for 20 days from July 29

to August 17, 2016, scaled to a standard deviation of $0.3 \cdot \sigma$, with added Gaussian noise of $0.2 \cdot \sigma$, where σ is the standard deviation of the original time series [48].

Given this input, each algorithm then returns a ranking of the anomalies. We evaluate this using standard metrics, AUC² (area under the ROC curve) and F-measure³ ($\frac{2 \cdot \text{precision} \cdot \text{recall}}{\text{precision} + \text{recall}}$), the latter computed on the top 50 anomalies output by each algorithm.

Baselines: Dynamic graph anomaly detection approaches [31], [32], [34], [49] cannot be used as they consider graph structure only, but not sensor data. [33] allows sensor data but requires graphs with fully observed edge weights, which is inapplicable as detecting failed power lines with all sensors present reduces to checking if any edge has current equal to 0. Hence, instead, we compare DYNWATCH to GridWatch [27], an anomaly detection approach for sensors on a static graph, and the following multidimensional time-series based anomaly detection methods: Isolation Forests [26], Vector Autoregression (VAR) [21], Local Outlier Factor (LOF) [24], and Parzen Window [50]. Each uses the currents and voltages at the given sensors as features. For VAR, the norms of the residuals are used as anomaly scores; the remaining methods return anomaly scores directly.

For Isolation Forests, we use 100 trees (following the defaults in scikit-learn [51]). For VAR, following standard practice, we select the order by maximizing AIC. For LOF we use 20 neighbors (following the default in scikit-learn), and we use 20 neighbors for Parzen Window.

As shown in Figure 6, DYNWATCH clearly outperforms the baselines on both metrics, having an F-measure of 21% to 25% higher than the best baseline.

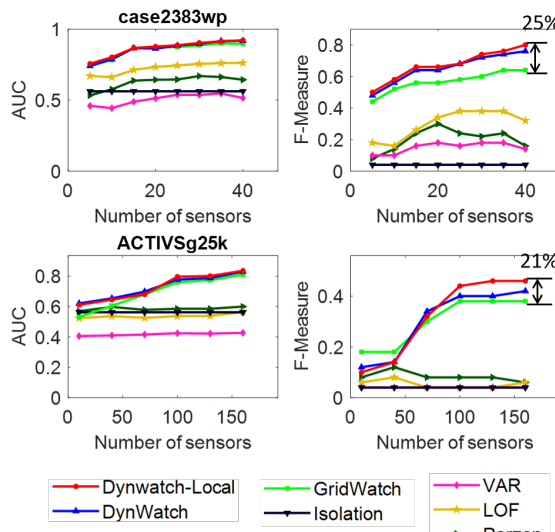


Fig. 6. Experiment results by AUC and F-measure

²AUC is the probability of correct ranking of a random “positive” “negative” pair.

³F-measure is a trade-off between precision and recall.

B. Q2. Scalability

In this subsection, we seek to analyze the scalability of our DYNWATCH and DYNWATCH-LOCAL. In reality, PJM, the largest ISO in the U.S., runs ACSE on a 28k bus model, performed every 1 min [52], thus any anomaly detection algorithm that takes significantly less than 1 min may provide valuable information to prevent wrong control decisions in real-time. The following results demonstrate the proposed method’s capability to achieve this.

Here, we generate testcases of different sizes by starting with the CASE2383 case and duplicating it 3, 4, 5, ..., 12 times. After each duplication, edges are added to connect each node with its counterpart in the last duplication, so that the whole grid is connected. Then for each testcase, we generate 20 dynamic grids and sensor data with 1 randomly chosen sensor and 1200 time ticks, following the same settings as the previous sub-section. Finally, we measure the time taken for the whole DYNWATCH and DYNWATCH-LOCAL methods.

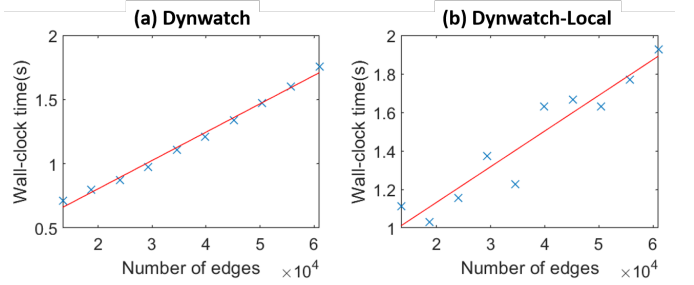


Fig. 7. Our algorithms scale linearly: wall-clock time of (a) DYNWATCH; and (b) DYNWATCH-LOCAL against number of edges, when detecting on all 1200 time ticks. The red lines are best-fit regression lines.

Figure 7 shows that our method is fast: even on a large case with 60k+ branches, both methods took less than 2s to apply anomaly detection on all 1200 time ticks of the sensor, corresponding to an average of less than 1.7ms per time tick per sensor. The ACTIVSG25K (similar to the largest real-time network in the US) has 32k+ branches, and thus run-time of anomaly detection at each time t will be significantly less than 1 min. The figure also shows that our methods scale close to linearly with the grid size.

V. CONCLUSION

In this paper, we proposed DYNWATCH, an online algorithm that accurately detects anomalies using sensor data on a changing graph (grid). DYNWATCH applies a similarity-based approach to measure how much the graph changes over time, with which we assign greater weight to previous graphs which are similar to the current graph. We use a domain-aware graph similarity measure based on Line Outage Distribution Factors (LODF), which exploit physics-based modeling of how changes in one line affect other lines in the graph.

By plugging in different graph similarity measures, our approach could be applied to other domains. Hence, future work could study how sensitive various detectors are for detecting anomalies in graph-based sensor data from different domains.

- 1) **Problem Formulation and Algorithm:** we propose a novel and practical problem formulation, of anomaly detection using sensors on a changing graph. For this problem, we propose a graph-similarity based approach, and a domain-aware similarity measure based on Line Outage Distribution Factors (LODF).
- 2) **Effectiveness:** Our DYNWATCH algorithm outperforms existing approaches in accuracy by 20% or more (F-measure) in experiments.
- 3) **Scalability:** DYNWATCH is fast, taking 1.7ms on average per time tick per sensor on a 60k edge graph, and scaling linearly in the size of the graph.

Reproducibility: our code and data are publicly available at <https://github.com/bhooi/dynamic.git>.

REFERENCES

- [1] S. M. Amin, "Us grid gets less reliable [the data]," *IEEE Spectrum*, vol. 48, no. 1, pp. 80–80, 2011.
- [2] N. Perforth, "Hackers are targeting nuclear facilities, homeland security dept. and fbi say," *New York Times*, vol. 6, 2017.
- [3] D. U. Case, "Analysis of the cyber attack on the ukrainian power grid," *Electricity Information Sharing and Analysis Center (E-ISAC)*, vol. 388, 2016.
- [4] R. M. Lee, M. Assante, and T. Conway, "Crashoverride: Analysis of the threat to electric grid operations," *Dragos Inc.*, March, 2017.
- [5] F. Maghsoudlou, R. Masiello, and T. Ray, "Energy management systems," *IEEE Power and Energy Magazine*, vol. 2, no. 5, pp. 49–57, 2004.
- [6] F. C. Schweppe and J. Wildes, "Power system static-state estimation, part i: Exact model," *IEEE Transactions on Power Apparatus and Systems*, no. 1, pp. 120–125, 1970.
- [7] E. Handschin, F. C. Schweppe, J. Kohlas, and A. Fiechter, "Bad data analysis for power system state estimation," *IEEE Transactions on Power Apparatus and Systems*, vol. 94, no. 2, pp. 329–337, 1975.
- [8] M. Göl and A. Abur, "Lav based robust state estimation for systems measured by pmus," *IEEE Transactions on Smart Grid*, vol. 5, no. 4, pp. 1808–1814, 2014.
- [9] L. Mili, V. Phaniraj, and P. J. Rousseeuw, "Least median of squares estimation in power systems," *IEEE Transactions on Power Systems*, vol. 6, no. 2, pp. 511–523, 1991.
- [10] R. C. Pires, A. S. Costa, and L. Mili, "Iteratively reweighted least-squares state estimation through givens rotations," *IEEE Transactions on Power Systems*, vol. 14, no. 4, pp. 1499–1507, 1999.
- [11] S. Li, A. Pandey, and L. Pileggi, "A wlav-based robust hybrid state estimation using circuit-theoretic approach," *arXiv preprint arXiv:2011.06021*, 2020.
- [12] Y. Weng, M. D. Ilić, Q. Li, and R. Negi, "Convexification of bad data and topology error detection and identification problems in ac electric power systems," *IET Generation, Transmission & Distribution*, vol. 9, no. 16, pp. 2760–2767, 2015.
- [13] A. Jovicic, M. Jereminov, L. Pileggi, and G. Hug, "An equivalent circuit formulation for power system state estimation including pmus," in *2018 North American Power Symposium (NAPS)*. IEEE, 2018, pp. 1–6.
- [14] S. Li, A. Pandey, S. Kar, and L. Pileggi, "A circuit-theoretic approach to state estimation," in *2020 IEEE PES Innovative Smart Grid Technologies Europe (ISGT-Europe)*, 2020, pp. 1126–1130.
- [15] A. Monticelli, *State estimation in electric power systems: a generalized approach*. Springer Science & Business Media, 2012.
- [16] M. Prais and A. Bose, "A topology processor that tracks network modifications," *IEEE Transactions on Power Systems*, vol. 3, no. 3, pp. 992–998, 1988.
- [17] O. Alsac, N. Vempati, B. Stott, and A. Monticelli, "Generalized state estimation," *IEEE Transactions on power systems*, vol. 13, no. 3, pp. 1069–1075, 1998.
- [18] F. F. Wu and W.-H. Liu, "Detection of topology errors by state estimation (power systems)," *IEEE Transactions on Power Systems*, vol. 4, no. 1, pp. 176–183, 1989.
- [19] E. M. Lourenço, E. P. Coelho, and B. C. Pal, "Topology error and bad data processing in generalized state estimation," *IEEE Transactions on Power Systems*, vol. 30, no. 6, pp. 3190–3200, 2014.
- [20] B. Donmez, G. Scioletti, and A. Abur, "Robust state estimation using node-breaker substation models and phasor measurements," in *2019 IEEE Milan PowerTech*. IEEE, 2019, pp. 1–6.
- [21] J. D. Hamilton, *Time series analysis*. Princeton university press Princeton, 1994, vol. 2.
- [22] Z. Wang, J. Yang, Z. ShiZe, and C. Li, "Robust regression for anomaly detection," in *2017 IEEE International Conference on Communications (ICC)*. IEEE, 2017, pp. 1–6.
- [23] S. Yi, J. Ju, M.-K. Yoon, and J. Choi, "Grouped convolutional neural networks for multivariate time series," *arXiv preprint arXiv:1703.09938*, 2017.
- [24] M. M. Breunig, H.-P. Kriegel, R. T. Ng, and J. Sander, "Lof: identifying density-based local outliers," in *ACM sigmod record*, vol. 29, no. 2. ACM, 2000, pp. 93–104.
- [25] M. Amer and S. Abdennadher, "Comparison of unsupervised anomaly detection techniques," *Bachelor's Thesis*, 2011.
- [26] F. T. Liu, K. M. Ting, and Z.-H. Zhou, "Isolation forest," in *ICDM*. IEEE, 2008, pp. 413–422.
- [27] B. Hooi, D. Eswaran, H. A. Song, A. Pandey, M. Jereminov, L. Pileggi, and C. Faloutsos, "Gridwatch: Sensor placement and anomaly detection in the electrical grid," in *ECML-PKDD*. Springer, 2018, pp. 71–86.
- [28] E. Keogh, J. Lin, S.-H. Lee, and H. Van Herle, "Finding the most unusual time series subsequence: algorithms and applications," *Knowledge and Information Systems*, vol. 11, no. 1, pp. 1–27, 2007.
- [29] S. Ramaswamy, R. Rastogi, and K. Shim, "Efficient algorithms for mining outliers from large data sets," in *ACM Sigmod Record*, vol. 29, no. 2. ACM, 2000, pp. 427–438.
- [30] M. Jones, D. Nikovski, M. Imamura, and T. Hirata, "Anomaly detection in real-valued multidimensional time series," in *International Conference on Bigdata/Socialcom/Cybersecurity*. Stanford University, ASE. Cite-seer, 2014.
- [31] L. Akoglu, M. McGlohon, and C. Faloutsos, "Oddball: Spotting anomalies in weighted graphs," in *PAKDD*. Springer, 2010, pp. 410–421.
- [32] Z. Chen, W. Hendrix, and N. F. Samatova, "Community-based anomaly detection in evolutionary networks," *Journal of Intelligent Information Systems*, vol. 39, no. 1, pp. 59–85, 2012.
- [33] M. Mongiovì, P. Bogdanov, R. Ranca, E. E. Papalexakis, C. Faloutsos, and A. K. Singh, "Netspot: Spotting significant anomalous regions on dynamic networks," in *SDM*. SIAM, 2013, pp. 28–36.
- [34] M. Araujo, S. Papadimitriou, S. Günemann, C. Faloutsos, P. Basu, A. Swami, E. E. Papalexakis, and D. Koutra, "Com2: fast automatic discovery of temporal ('comet') communities," in *PAKDD*. Springer, 2014, pp. 271–283.
- [35] L. Akoglu and C. Faloutsos, "Event detection in time series of mobile communication graphs," in *Army science conference*, 2010, pp. 77–79.
- [36] C. C. Aggarwal, Y. Zhao, and S. Y. Philip, "Outlier detection in graph streams," in *Data Engineering (ICDE), 2011 IEEE 27th International Conference on*. IEEE, 2011, pp. 399–409.
- [37] S. Ranshous, S. Harenberg, K. Sharma, and N. F. Samatova, "A scalable approach for outlier detection in edge streams using sketch-based approximations," in *SDM*. SIAM, 2016, pp. 189–197.
- [38] J. Valenzuela, J. Wang, and N. Bissinger, "Real-time intrusion detection in power system operations," *IEEE Transactions on Power Systems*, vol. 28, no. 2, pp. 1052–1062, 2012.
- [39] R. Mitchell and R. Chen, "Behavior-rule based intrusion detection systems for safety critical smart grid applications," *IEEE Transactions on Smart Grid*, vol. 4, no. 3, pp. 1254–1263, 2013.
- [40] S. Papadimitriou, J. Sun, and C. Faloutsos, "Streaming pattern discovery in multiple time-series," 2005.
- [41] P. Galeano, D. Peña, and R. S. Tsay, "Outlier detection in multivariate time series by projection pursuit," *Journal of the American Statistical Association*, vol. 101, no. 474, pp. 654–669, 2006.
- [42] R. Baragona and F. Battaglia, "Outliers detection in multivariate time series by independent component analysis," *Neural computation*, vol. 19, no. 7, pp. 1962–1984, 2007.
- [43] H. Lu, Y. Liu, Z. Fei, and C. Guan, "An outlier detection algorithm based on cross-correlation analysis for time series dataset," *IEEE Access*, vol. 6, pp. 53 593–53 610, 2018.
- [44] A. Blázquez-García, A. Conde, U. Mori, and J. A. Lozano, "A review on outlier/anomaly detection in time series data," *arXiv preprint arXiv:2002.04236*, 2020.
- [45] D. J. Brueni and L. S. Heath, "The pmu placement problem," *SIAM Journal on Discrete Mathematics*, vol. 19, no. 3, pp. 744–761, 2005.
- [46] A. J. Wood, B. F. Wollenberg, and G. B. Sheblé, *Power generation, operation, and control*. John Wiley & Sons, 2013.

- [47] R. D. Zimmerman, C. E. Murillo-Sánchez, and R. J. Thomas, “Matpower: Steady-state operations, planning, and analysis tools for power systems research and education,” *IEEE Transactions on power systems*, vol. 26, no. 1, pp. 12–19, 2011.
- [48] H. A. Song, B. Hooi, M. Jereminov, A. Pandey, L. Pileggi, and C. Faloutsos, “Powercast: Mining and forecasting power grid sequences,” in *ECML-PKDD*. Springer, 2017, pp. 606–621.
- [49] N. Shah, D. Koutra, T. Zou, B. Gallagher, and C. Faloutsos, “Time-crunch: Interpretable dynamic graph summarization,” in *KDD*. ACM, 2015, pp. 1055–1064.
- [50] E. Parzen, “On estimation of a probability density function and mode,” *The annals of mathematical statistics*, vol. 33, no. 3, pp. 1065–1076, 1962.
- [51] F. Pedregosa, G. Varoquaux, A. Gramfort, V. Michel, B. Thirion, O. Grisel, M. Blondel, P. Prettenhofer, R. Weiss, V. Dubourg, J. Vanderplas, A. Passos, D. Cournapeau, M. Brucher, M. Perrot, and E. Duchesnay, “Scikit-learn: Machine learning in Python,” *Journal of Machine Learning Research*, vol. 12, pp. 2825–2830, 2011.
- [52] “Pjm manual 12: Balancing operations,” <https://www.pjm.com/~/media/documents/manuals/m12.ashx>, 2020.